Adsorption of pharmaceutical pollutants onto graphene nanoplatelets

Lateefa A. Al-Khateeb [a], Sitah Almotiry [a,b], Mohamad Abdel Salam [a,*]

[a] Chemistry Department, Faculty of Science, King Abdulaziz University, P.O. Box 80200, Jeddah 21589, Saudi Arabia
[b] Center of Excellence in Environmental Studies, King Abdulaziz University, P.O. Box 80216, Jeddah 21589, Saudi Arabia

HIGHLIGHTS

- Removal of hazardous pharmaceutical pollutants by graphene nanoplatelets (GNPs) was studied.
- The effects of adsorption parameters were studied and optimized.
- The adsorption was studied kinetically and thermodynamically.
- GNPs were used for the removal of the PPs from real environmental samples.

GRAPHICAL ABSTRACT

This graph show the adsorption of aspirin (ASA), caffeine (CAF), and acetaminophen (APAP), from Red Sea water (RSW), waste water (WW), and TAP water (TW), samples spiked with 20 mg/l, by GNPs.
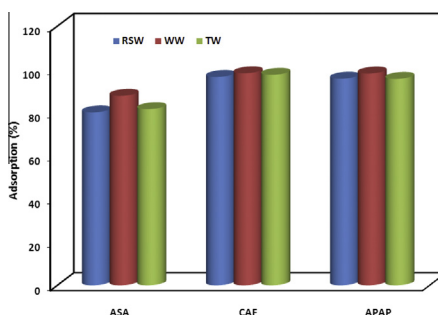
ABSTRACT

This study explores the removal of aspirin (ASA), acetaminophen (APAP), and caffeine (CAF); as examples of hazardous pharmaceutical pollutants, from aqueous solution by graphene nanoplatelets (GNPs). Characterization of the GNPs showed a transparent, layered structure with a smooth surface and many wrinkles, as well as a specific surface area of 635.2 $m^2 g^{-1}$. The effects of adsorption time, GNPs mass, solution pH, ionic strength, and temperature were studied and optimized. The effect of temperature on the adsorption kinetics was investigated using pseudo-first-order, pseudo-second-order kinetic models, and the experimental data were fitted well to the pseudo-second-order kinetic model. Also, the adsorption mechanism was explored using intra-particle diffusion and liquid film diffusion models, and the results revealed that none of these models was the rate-determining steps. The adsorption was studied thermodynamically, and the Gibbs free energy change ($\Delta G°$), enthalpy change ($\Delta H°$), and entropy change ($\Delta S°$), were calculated. The $\Delta G°$ values were negative at all temperatures indicating the spontaneity of the adsorption of ASA, APAP, and CAF by GNPs from aqueous solution. GNPs showed great efficiency when they were used for the removal of ASA, APAP, and CAF from real environmental samples.

© 2014 Elsevier B.V. All rights reserved.

1. Introduction

Pharmaceutical pollutants (PPs) are a group of emerging anthropogenic hazard contaminants that contain different groups of human and veterinary medicinal compounds that are used widely all over the globe. PPs exist in the environment at a very low concentration but, generally due to their bio-accumulation, they pose a potential long-term risk for aquatic and terrestrial organisms. Therefore, over the past few years, PPs have been considered an emerging environmental problem. Usually, pharmaceutical compounds are designed to affect humans and animals

* Corresponding author. Tel.: +966 541886660; fax: +966 2 6952292.
E-mail address: masalam16@hotmail.com (M.A. Salam).

physiologically in very low concentrations. Since very low concentrations of pharmaceuticals may cause subtle, chronic effects on ecosystems, the totality of their ecotoxicological impacts on the aquatic environment over the long term is difficult to predict [1]. Pharmaceutical compounds are resistant to biological degradation and retain their chemical structure long enough to do their adverse effect [2]. The pharmaceutical pollutants most frequently found in water treatment effluents are antibiotics, antacids, steroids, antidepressants, analgesics, anti-inflammatories, antipyretics, beta-blockers, lipid-lowering drugs, tranquilizers, and stimulants. Currently, there are various methods used for the removal of conventional pollutants from polluted water, such as submerged membrane bioreactor [3] activated sludge treatment [4], constructed wetland [5], photocatalytic oxidation [6], catalytic ozonation [7], or adsorption [8,9], but they cannot be used effectively to remove pharmaceutical pollutants from water effluents [10]. Therefore, effective treatments are needed for this emerging class of pollutants. Of the above mentioned methods, adsorption is the most promising method for the removal of pollutants because both water and the adsorbent could be recycled, and no by-products would be produced. Hence, scientists continuously search for new types of adsorbents and to develop new efficient removal methods.

Graphene is a new fascinating carbon material that has attracted the attention of scientist in recent years. It is a one-atom-thick, two-dimensional (2D) layer of sp^2-bonded carbon. Graphene also exhibits extraordinary properties, such as excellent mechanical, electrical, thermal, optical properties and very high specific surface area. Additionally, graphene has also been used as an excellent adsorbent for different pollutants [11–15] due to its large, delocalized π-electron system, which can form strong interactions with other pollutants.

In this study, high surface area graphene nanoplatelets were used for the first time to adsorb/remove a group of the most frequently used pharmaceutical compounds, aspirin (or acetylsalicylic acid), acetaminophen (N-acetyl-para-aminophenol), and caffeine (1,3,7-trimethyl-1H-purine-2,6(3H,7H)-dione 3,7-dihydro-1,3,7-trimethyl-1H-purine-2,6-dione). Aspirin (ASA) is the most frequently used non-steroidal anti-inflammatory drug, whereas acetaminophen (APAP) is used to reduce pain and fever. Caffeine (CAF) is a central nervous system stimulant, which presents in many analgesic drugs. The effects of different adsorption conditions were studied: solution pH, temperature, and adsorption time. Additionally, the adsorption process was studied kinetically to predict the adsorption rate in order to understand the adsorption behavior. Also, the adsorption was studied thermodynamically to understand the mechanism of adsorption and its spontaneity by calculating different thermodynamic parameters.

2. Materials and methods

2.1. Materials

Graphene nanoplatelets (GNPs) were obtained from XG Science (xGnP®-C-750), USA. xGnP® Graphene Nanoplatelets are unique nanoparticles consisting of short stacks of graphene sheets having a platelet shape with thickness ranging from 1 to 20 nm and width ranging from 1 to 50 μm. The pharmaceutical drugs; aspirin, acetaminophen, and caffeine, were obtained from Sigma–Aldrich Canada (laboratory reagent grade). All other chemicals were obtained from Sigma–Aldrich (analytical grade) and all solutions were prepared using deionized water. A stock solution of 1000 mg/l containing ASA, CAF, and APAP was prepared by dissolving 10 mg from each chemical in 10 ml deionized water. 0.1 M NaOH was prepared by dissolving 4.0 g in 100 ml deionized water, and

diluting 0.83 ml of concentrated nitric acid (37.2%, sp. gr. 1.19) to 100.0 ml with deionized water.

2.2. Characterization techniques

Transmission Electron Microscopy (TEM) measurements of the graphene nanoplatlets was made with a JEOL JEM 2100FX microscope operating at 200 keV, point resolution of 0.31 nm. The specimens for analysis were prepared by dispersing the powdered sample in ethanol using an ultrasonic bath. A drop of each resulting suspension was placed on a copper grid covered with a porous carbon film. X-ray diffraction (XRD) analysis was performed with an X-ray diffractometer from X'Pert Pro PANalytical. Bragg's angles (2θ) between 20 and 60° were recorded at a rate of 0.04° per step with 20 s per step. Textural properties were evaluated by means of N_2 adsorption–desorption isotherms recorded at liquid N_2 temperature with a Micromeritics ASAP 2000 apparatus. Samples were degassed at 150 °C under vacuum for 24 h. Specific areas were calculated by applying the BET equation within the relative pressure range $P/P^0 = 0.05–0.30$ [16].

2.3. Analytical method

Aspirin, caffeine, and acetaminophen concentrations were measured using HPLC (Hewlett Packard 1100 series liquid chromatograph (Avondale, CA)). The HPLC system consisted of two pumps and UV detector. Separations were achieved on analytical reversed phase C18 column (4.6 × 150 mm, 5 μm) at a mobile phase flow rate of 1 ml/min under isocratic conditions a mixture of water/acetonitrile/triethylamine/acetic acid (84.6:15:0.2:0.2; v/v/v/v). The sample size injected was 10 μl and UV detection wavelength was 254 nm and the chromatogram is presented in Fig. 1.

2.4. Adsorption experiments

Adsorption experiments were carried out to explore the effect of adsorption parameters; adsorption time, adsorbent mass, solution pH, ionic strength, and solution temperature. A series of 10.0 ml solutions containing 20.0 mg l⁻¹ of ASA, CAF, and APAP, were prepared in 25.0 ml glass bottle and kept at a certain temperature, (2) the pH of the solution was adjusted using 0.1 M NaOH and 0.1 M HCl, and then certain amount of the GNPs were added into the solution. The solution was shaked continuously for a certain period of time, then after the completion of preset time intervals; the solution was filtered immediately through a filter paper (Whatman® quantitative filter paper, ashless, Grade 42, 2.5 μm)) to collect the supernatant. The residual of ASA, CAF, and APAP concentrations in the aqueous solution were then determined by HPLC and prior to injection the solution was filtered through 0.45 μm syringe filter (Cellulose Acetate), to be sure that the injected solution is free from any GNPs, to avoid the blockage of the HPLC column, and misleading results. The % adsorbed by both filter paper and syringe filter was less than 2%. The percentage adsorption in solution was calculated using Eq. (1):

$$\% \text{ Adsorption} = \frac{(C_o - C_t)}{C_o} \times 100 \qquad (1)$$

where C_0 is the initial concentration (mg/l), C_t is the final concentration after a certain period of time (mg/l). The adsorption kinetics was studied to identify adsorption rate and mechanism. Kinetic experiments were carried out by mixing 200.0 mg GNPs with 200.0 ml of 20.0 mg/l ASA, CAF, and APAP and the solution pH was adjusted to 8.0 using 0.1 M NaOH/0.1 M HCl solutions. The samples were withdrawn at predetermined time, filtered, and the residual concentrations of ASA, CAF, and APAP were measured.
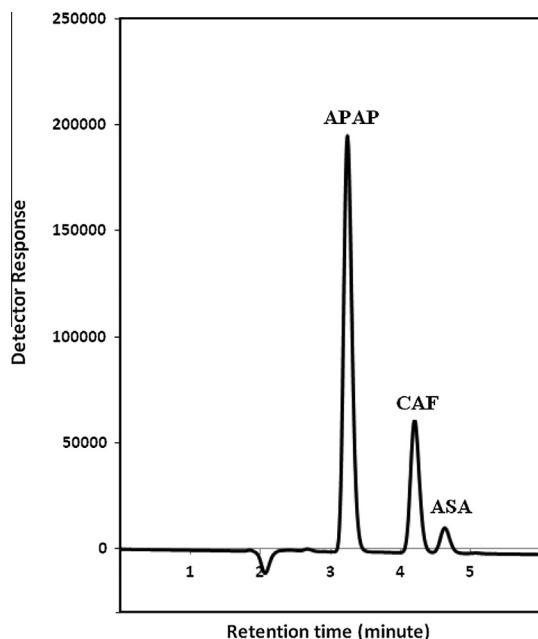
Fig. 1. HPLC-UV chromatogram of ASA, CAF, and APAP.

The adsorption capacity at any time was calculated according to the following equation:

$$q_t = \frac{(C_o - C_t)V}{m} \qquad (2)$$

where q_t is the amount of ASA, CAF, and APAP adsorbed by the GNPs (mg/g), V is the initial solution volume (L) and m is the GNPs mass (g).

It is noteworthy to mention that each experiment was performed in triplicate and the reported values are the average of the three measurements. Also, the adsorption of ASA, CAF, and APAP by the glassware's and filter paper was determined by running a blank experiment without GNPs and was found to be negligible.

2.5. Real water samples

Two real samples were used to study the efficiency of GNPs for the removal of ASA, CAF, and APAP. A tap water sample (TWS) was collected from our lab after allowing the tap water to flow for 10 min. The wastewater sample (WWS) was collected from the waste water treatment plant at King Abdulaziz University, Jeddah City. Both samples were filtered through 0.45 μm Millipore filter paper and kept in Teflon® bottles at 5 °C in the dark. The properties of the three real water samples are tabulated in Table 1.

Table 1
Analysis of the Red Sea water, waste water, and tap water samples.

	RSWS	WWS	TWS
Collection date	25/3/2013	06/4/2013	18/4/2013
pH	7.6	7.01	8.85
TDS (mg/l)	39,000	1112	108
Conductivity (μS/cm)	78,000	1593	169
TSS (mg/l)	2	1	Nil
COD (mg/l)	184	6	Nil
BOD (mg/l)	36.3	3.5	Nil
Na+ (mg/l)[a]	16,561	205	109
Ca2+ (mg/l)[a]	738.4	66.57	88
Mg2+ (mg/l)[a]	1987	14	14

[a] Measured with an Optima 4300TM DV ICP-OES (PerkinElmer®).

3. Results and discussion

3.1. Characterization of GNPs

A transmission electron microscope (TEM) was used to characterize the graphene nanoplatelets by their morphological structure. As seen in Fig. 2, GNPs exhibit a transparent, layered structure with a smooth surface and many wrinkles. Fig. 3 showed the XRD pattern of graphene nanoplatelets with diffraction peaks corresponding to (002) and (100) planes characteristics of GNPs [17]. Usually, the adsorption process greatly depends on the specific surface area of the solid adsorbent. Therefore, it is crucial to measure the specific surface area of the GNPs using nitrogen adsorption/desorption isotherms. The adsorption isotherms were determined from N_2 adsorption measured at 77 K and the results were presented in Fig. 4. The isotherm obtained was classified as a type IV isotherm with an H3 type hysteresis loop according to the original IUPAC classification and corresponding to solids with platelike particles [18]. The specific surface area for the GNPs was calculated from the BET equation and was found to be 635.2 $m^2 \, g^{-1}$.

3.2. Adsorption study

Adsorption of organic pollutants such as ASA, CAF, and APAP from aqueous solutions by carbon-based adsorbents might be governed by non-electrostatic interactions, and predominantly by Van der Waals interactions. However, there are many other, minor factors that affect this type of interaction and consequently affect the adsorption process. These factors include adsorption time, adsorbent mass, and solution conditions including pH, ionic strength, and temperature. Accordingly, the effect of different factors on the interaction between GNPs and ASA, CAF, and APAP was explored and studied.

The effect of GNP mass on the adsorption profile of ASA, CAF, and APAP was studied using 2.0, 5.0, 10.0, 15.0, 20.0 mg, and the % adsorption was 25.0%, 44.6%, 62.3%, 79,1%, 94.3%, for ASA, 82.1%, 97.3%, 98.4%, 99.2%, 99.5%, for CAF, and 55.3%, 76.8%, 84.5%, 97,1%, 98.3%, for APAP, respectively. Generally, it was observed that the percentage of ASA, CAF, and APAP adsorption
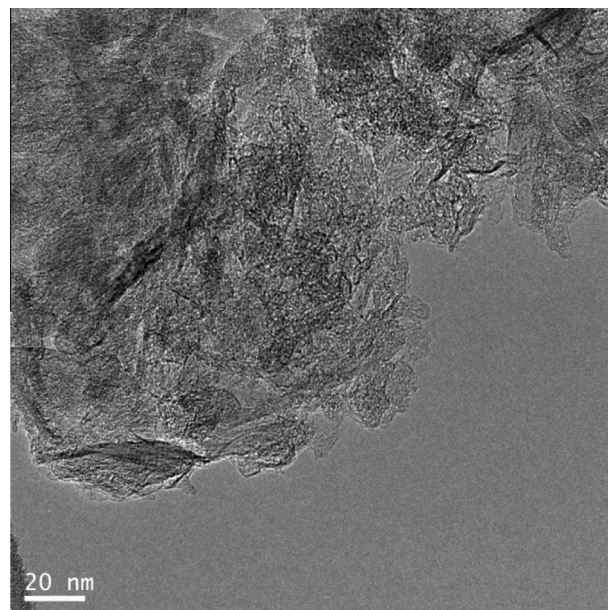

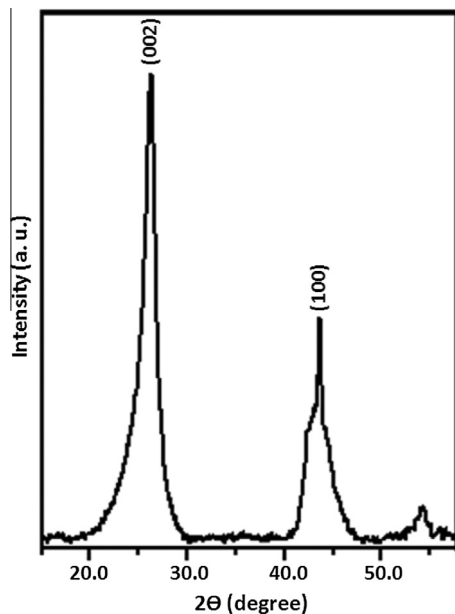**Fig. 2.** Transmittance electron microscope image for the GNPs.
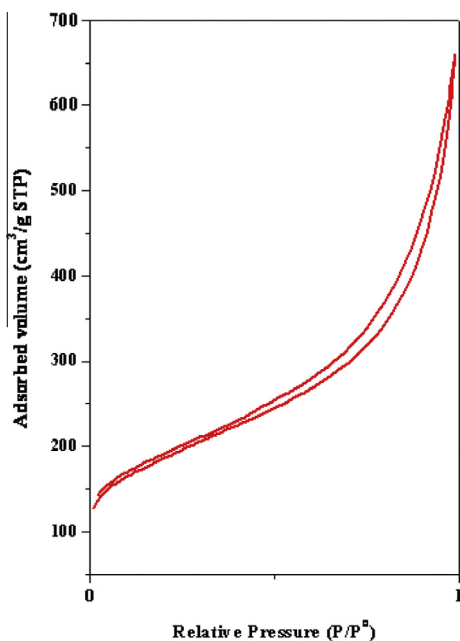
Fig. 3. XRD pattern for the GNPs.

Fig. 4. Nitrogen adsorption/desorption isotherms for GNPs.

Fig. 5. The effect of adsorption time on the adsorption of ASA, CAF, and APAP by GNPs from model solution. (Experimental conditions: 10.0 ml, pH 8.0, 4.0 mM KNO_3, 10.0 mg GNPs, 296 K, and ASA, CAF, and APAP concentrations 20.0 mg l^{-1}.)

Fig. 6. The effect of solution pH on the adsorption of ASA, CAF, and APAP by GNPs from model solution. (Experimental conditions: 10.0 ml, 60.0 min, 4.0 mM KNO_3, 10.0 mg GNPs, 296 K, and ASA, CAF, and APAP concentrations 20.0 mg l^{-1}.)

increased almost linearly with the increase of GNP mass until an adsorbent mass of 15.0 mg was used. Increases in GNP mass beyond 15.0 mg slightly affect adsorption, as most of the ASA, CAF, and APAP had already been adsorbed. This trend is mostly attributed to the increase in the adsorption surface area due to the increase in GNP mass, and thus the availability of more active adsorption sites for the ASA, CAF, and APAP molecules. Once most of the ASA, CAF, APAP molecules were adsorbed, further increases of GNP mass did not affect the percentage of adsorption. Accordingly, further experiments were conducted using 10.0 mg of GNPs to be able to monitor the change in% adsorption upon the change in the other factors. Using 10.0 mg GNP% adsorption was 62.3% for ASA, 98.4% for CAF, and 84.5% for APAP.
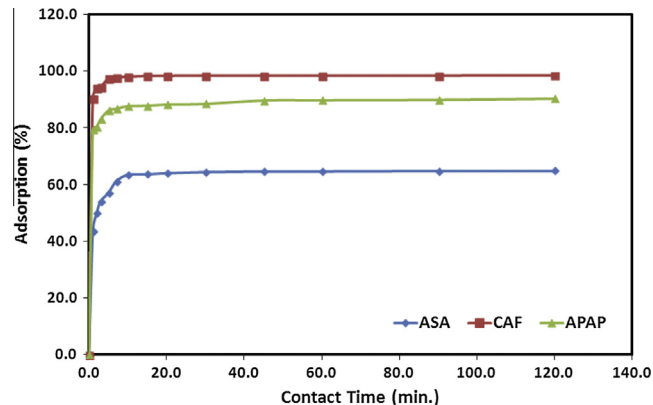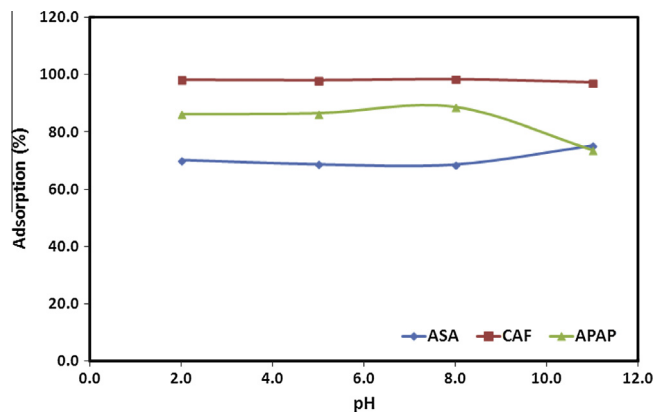
Fig. 5 shows the effect of adsorption time on the percentage of adsorption of ASA, CAF, and APAP by GNPs. The figure shows that the percentage of adsorption of these three pharmaceutical pollutants increased with time for the first 10 min. At this point, equilibrium was achieved, with adsorption of 63.5%, 94.3%, and 87.6%, for ASA, CAF, respectively. After 10 min, no further improvement in% adsorption was observed. Also, it is clear from the figure that ASA, CAF, and APAP adsorption occurred in two different stages. The first stage occurred during the first 10 min of adsorption, and was characterized by the high number of active binding sites on the GNPs surface during this phase. Adsorption occurred rapidly in this step, which indicates that the adsorption was controlled by the diffusion process of the ASA, CAF, and APAP molecules from the bulk phase to the GNPs surface. In the second step, adsorption was most likely an attachment-controlled process due to the decrease in the number of active sites available for the ASA, CAF, and APAP molecules on the GNPs' surface. For further experiments, 60 min of adsorption time was selected to ensure that equilibrium was attained for the adsorption of ASA, CAF, and APAP by GNPs.

The effect of pH on the removal efficiencies of ASA, CAF, and APAP by GNPs at pH values from 2.0 to 11.0 was explored and the results are presented in Fig. 6. In general, the removal of pharmaceutical compounds by GNPs was not dependent on the pH of the solution in the case of ASA and CAF; the percentage of adsorption (70% and 80%, respectively) was not changed significantly by altering the pH value. In the case of APAP, increasing the pH from

2.0 to 8.0 did not change the percentage of adsorption, but further increases of the pH, up to 11.0, were associated with a sudden decrease in the percentage of adsorption from 88.7% to 73.8%. This may be attributed to electrostatic repulsion between the negatively charged APAP ions; the pK_a value of APAP is 9.9 [19] and the GNPs covered by the negative hydroxide ions.

It is well known that ionic strength may affect the electrostatic and hydrophobic interactions between the adsorbate and the solid adsorbent. Thus, it is crucial to study the effect of ionic strength on the adsorption behavior of ASA, CAF, and APAP by GNPs. The influence of ionic strength on the adsorption of pharmaceutical compounds is significant, as it creates different adsorption situations in which the electrostatic interactions between the GNPs' surface and the pharmaceutical compounds are either attractive or repulsive. Ionic strength was adjusted in this study by adding concentrated KNO_3 to the solution containing ASA, CAF, and APAP, and the final concentrations of KNO_3 were 0.001, 0.002, 0.004 and 0.008 M, respectively. As it is presented in Fig. 7, the percentage of adsorption of ASA by GNPs was not altered by an increase in the ionic strength of the solution. This indicates that electrostatic interaction is not involved in the overall adsorption process. Meanwhile, the percentage of adsorption of CAF was slightly enhanced by increasing the KNO_3 concentration in the solution, and this indicates an enhancement in electrostatic attraction due to π–π stacking between the neutral CAF (pK_a = 14.0) and the GNPs' surface. On the other hand, the percentage of adsorption of APAP was not significantly altered by an increase in KNO_3 from 0.001 to 0.004 M; the percentage of adsorption remained around 89.2% throughout this range. Further increases in KNO_3 to 0.008 M were accompanied by a significant decrease in the percentage of adsorption to 81.1%. This may be due to a hindering effect caused by the high concentration of positively charged potassium ions and/or by the competition between the other pollutants present in the solution for adsorption on the available binding sites.

3.3. Adsorption kinetics

The effect of solution temperature on adsorption behavior was studied kinetically to predict the adsorption rate and adsorption mechanism between pharmaceutical pollutants and GNPs. The effect of temperature on the removal of ASA, CAF, and APAP, from an aqueous solution by GNPs was studied kinetically and the results are presented in Fig. 8. This figure shows that raising the solution temperature is associated with significant decreases in adsorption of the pharmaceutical pollutants from the solution by GNPs. The percentage of adsorption of ASA was decreased from 64.8% to
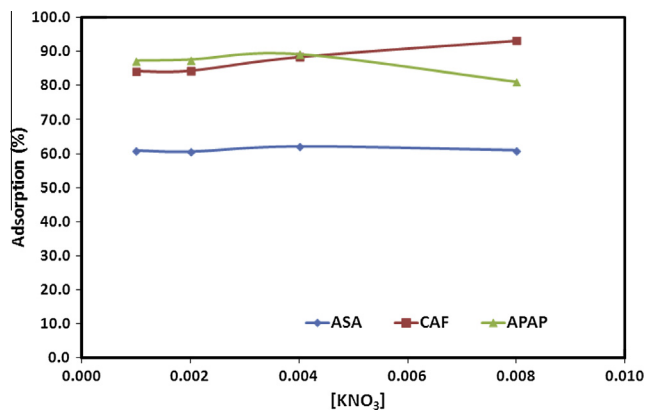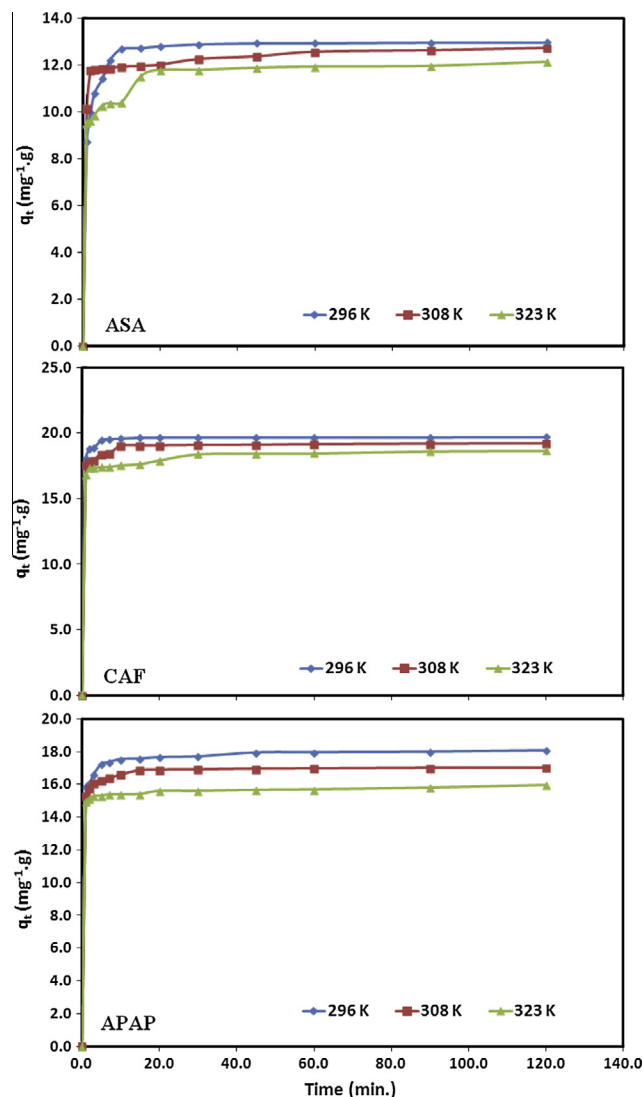
Fig. 8. The effect of solution temperature on the adsorption capacities (q_t) of ASA, CAF, and APAP by GNPs from model solution. (Experimental conditions: 200.0 ml, pH 8.0, 4.0 mM KNO_3, 200.0 mg GNPs, and ASA, CAF, and APAP concentrations 20.0 mg l^{-1}.)

63.6% and 60.7%, when the solution temperature was raised from 296 to 308 K, and 323 K, respectively. For CAF, the percentage of adsorption decreased from 98.5% to 96.0% and 93.2%. Adsorption of PAP decreased from 90.3% to 84.9% and 79.7%. The enhancement of the adsorption of ASA, CAF, and APAP by GNPs caused by lowering the solution temperature may indicate the exothermic nature of the adsorption process, which will be discussed in the thermodynamics section of this paper. From these experimental data, it was obvious that equilibrium adsorption capacity could be achieved after 5.0 min, as is presented in Fig. 8. Adsorption equilibrium was completely achieved within 20 min, which indicates the fast diffusion of pharmaceutical molecules from the liquid phase to the GNPs' surface. One significant, practical importance of this fast adsorption is the application of smaller reactor volumes, which ensure high efficiency and low cost. The maximum adsorption capacities reached for ASA, CAF, and APAP adsorbed on GNPs were 13.02 mg/g, 19.72 mg/g, and 18.06 mg/g, respectively, when the initial solution concentration was 20.0 mg/l, using 200 ml at 296 K and 200 mg GNPs.

In order to investigate the mechanisms of adsorption, various kinetic models have been suggested: pseudo-first-order,

Fig. 7. The effect of solution ionic strength on the adsorption of ASA, CAF, and APAP by GNPs from model solution. (Experimental conditions: 10.0 ml, 60.0 min, pH 8.0, 10.0 mg GNPs, 296 K, and ASA, CAF, and APAP concentrations 20.0 mg l^{-1}.)

pseudo-second-order kinetic models using Eqs. (3) and (4) based on Lagragen equation [20]:

$$\ln(q_e - q_t) = \ln \ q_e - k_1 t \tag{3}$$

$$\frac{t}{q_t} = \frac{1}{k_2 q_e^2} + \frac{t}{q_e} \tag{4}$$

where k_1 (min^{-1}) is the pseudo-first-order adsorption rate coefficient, k_2 g/(mg min) is the pseudo-second-order rate coefficient, and q_e and q_t are the values of the amount adsorbed per unit mass at equilibrium and at any time t, respectively. Plotting $\ln(q_e-q_t)$ vs. t for ASA, CAF, and APAP at different temperatures did not converge well and did not give straight lines with very low linear regression coefficients, as it is presented in Table 2. Meanwhile, applying the pseudo-second-order rate equation to the adsorption of ASA, CAF, and APAP experimental data converged very well, with excellent regression coefficients and straight lines, as is presented in Fig. 9. The parameters of the kinetic models were calculated from the experimental data, and the results of the pseudo-first-order and the pseudo-second-order kinetic parameters for ASA, CAF, and APAP adsorption by GNPs are presented in Table 2. Based on the values of the linear regression coefficients, the adsorption of ASA, CAF, and APAP by GNPs was found to be best described by the pseudo-second-order model ($R^2 > 0.99$). Also, the results showed that the amount adsorbed per unit mass of GNPs at equilibrium ($q_{e,calc}$), calculated from the slope of the pseudo-second-order plot, were in agreement with experimental values ($q_{e,exp}$), whereas this amount was underestimated by the pseudo-first-order model. These findings confirm the suitability of the pseudo-second-order rate equation for the description of ASA, CAF, and APAP adsorption by GNPs from aqueous solutions, and agreed well with previous studies. Carbon-based materials were used for the adsorption of acetaminophen kinetically and the adsorption data showed that the process follows the pseudo-second-order kinetic model [21]. Also, sepiolite was used for the removal of caffeine from aqueous solution and the adsorption process was found to obey the pseudo-second-order kinetic model [22].

3.4. Adsorption rate-controlling mechanism

Adsorption is a multi-step process involving the transport of the adsorbate molecules from the aqueous phase to the surface of the solid adsorbent particles followed by diffusion through the boundary layer to the external surface of the solid adsorbent; then the adsorption occurs at an active site on the solid adsorbent surface, and finally through intra-particle diffusion and adsorption through the solid adsorbent pores and aggregates. The intra-particle diffusion rate is expressed by the following equation [23]:

$$q_t = k_{id} t^{1/2} + C \tag{5}$$

where q_t is adsorption capacity at any time (t), k_{id} is the intra-particle diffusion rate constant (mg/g min$^{1/2}$), and C (mg/g) is a constant proportional to the thickness of the boundary layer. Plotting q_t vs. $t^{1/2}$ should converge and give a straight line. This line must pass through the origin if the adsorption process is controlled by the intra-particle diffusion. The experimental data of ASA, CAF, and APAP adsorption by GNPs at different temperatures were fitted using the intra-particle diffusion model, but they did not converge well and did not have straight lines that passed through the origin. In general, only the last part of the adsorption for all the kinetic data converged well with acceptable linear regression coefficients, as is shown in Table 2. This indicates that intra-particle diffusion is a part of the adsorption mechanism, but it is not the rate-determining step for the adsorption of ASA, CAF, and APAP by GNPS at different temperatures.

The liquid film diffusion model is another kinetic model that assumes the flow of the adsorbate molecules through a liquid film surrounded the solid adsorbent. The liquid film diffusion model can be expressed as follows:

$$\ln(1 - F) = -k_{fd} * t \tag{6}$$

where F is the fractional attainment of equilibrium ($F = q_t/q_e$) and k_{fd} (min^{-1}) is the film diffusion rate coefficient. Application of the liquid film diffusion model to the adsorption data of ASA, CAF, and APAP by GNPs at different temperatures did not converge well and the linear regression coefficients were very poor. The liquid film diffusion model was applied to the first 2 min in all kinetic data and,

Table 2
Different kinetic models parameters for the adsorption of Aspirin, acetaminophen, and caffeine by GNPs at different temperatures.

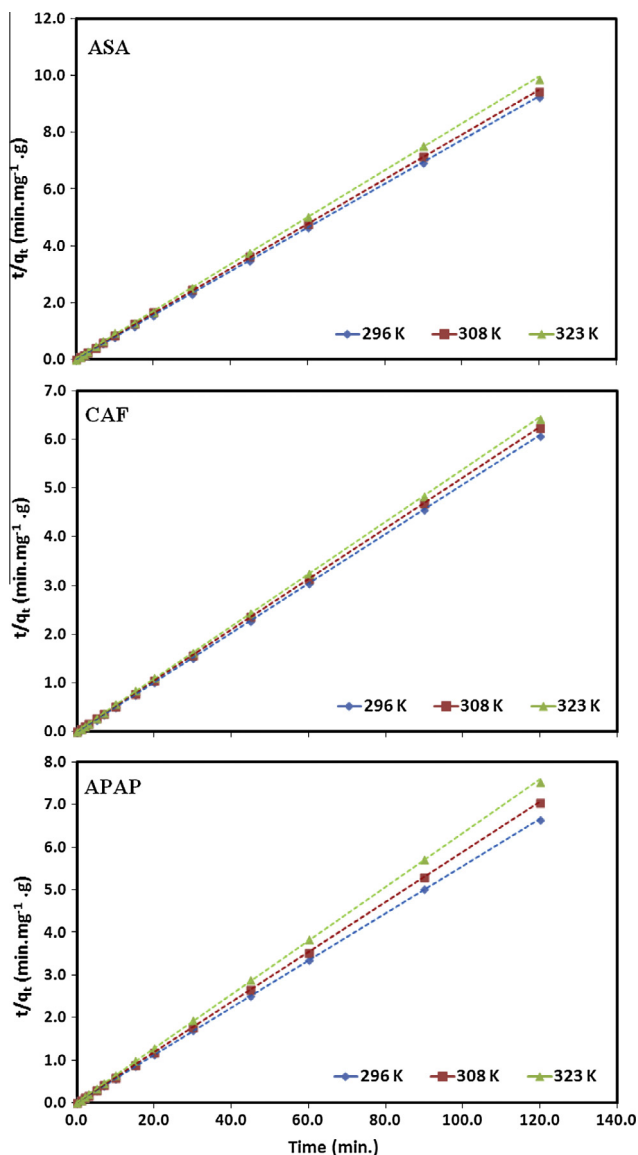| Acetaminophen					Caffeine					Aspirin				
Temperature	$q_{e,exp}$ (mg/g)	$q_{e,calc}$ (mg/g)	k_1	R^2	$q_{e,exp}$ (mg/g)	$q_{e,calc}$ (mg/g)	k_1	R^2	$q_{e,exp}$ (mg/g)	$q_{e,calc}$ (mg/g)	k_1	R^2
Pseudo-first-order kinetic model												
296 K	12.98	1.47	0.052	0.759	19.72	0.473	0.039	0.505	18.07	1.68	0.042	0.787
308 K	12.73	1.78	0.039	0.819	19.22	1.09	0.043	0.705	17.00	1.03	0.048	0.751
323 K	12.14	2.43	0.042	0.831	18.66	2.11	0.045	0.855	15.95	1.23	0.034	0.670
Temperature	$q_{e,exp}$ (mg/g)	$q_{e,calc}$ (mg/g)	k_2	R^2	$q_{e,exp}$ (mg/g)	$q_{e,calc}$ (mg/g)	k_2	R^2	$q_{e,exp}$ (mg/g)	$q_{e,calc}$ (mg/g)	k_2	R^2
Pseudo-second-order kinetic model												
296 K	12.98	13.02	0.188	0.999	19.72	19.72	0.777	0.999	18.07	18.07	0.185	0.999
308 K	12.73	12.71	0.138	0.999	19.22	19.22	0.303	0.999	17.00	17.02	0.331	0.999
323 K	12.14	12.14	0.105	0.999	18.66	18.67	0.127	0.999	15.95	15.88	0.211	0.999
Temperature	K_{id} (mg/g min$^{1/2}$)	C (mg/g)	R^2		K_{id} (mg/g min$^{1/2}$)	C (mg/g)	R^2		K_{id} (mg/g min$^{1/2}$)	C (mg/g)	R^2	
Intra-particle diffusion model												
296 K	9.33×10^{-3}	12.87	0.909		5.25×10^{-3}	19.65	0.874		8.09×10^{-2}	17.26	0.903	
308 K	1.09×10^{-1}	11.59	0.975		2.36×10^{-2}	18.95	0.987		2.11×10^{-2}	16.78	0.945	
323 K	5.04×10^{-2}	11.54	0.927		1.75×10^{-1}	17.03	0.883		7.44×10^{-2}	15.13	0.940	
Temperature	K_{fd} (min^{-1})	R^2			K_{fd} (min^{-1})	R^2			K_{fd} (min^{-1})	R^2		
Liquid film diffusion model												
296 K	0.335	0.945			1.43	0.875			0.815	0.774		
308 K	0.118	0.973			1.10	0.782			0.773	0.803		
323 K	0.784	0.758			1.01	0.817			0.704	0.764		

Fig. 9. Pseudo-second-order plots for ASA, CAF, and APAP adsorbed by GNPs at different temperatures. (Experimental conditions: 200.0 ml, pH 8.0, 4.0 mM KNO₃, 200.0 mg GNPs, and ASA, CAF, and APAP concentrations 20.0 mg l⁻¹.)

surprisingly, this data mostly converged with acceptable linear regression coefficients. This is presented in Table 2. This indicates that the liquid film diffusion controls the adsorption process within only the first 2 min in general, but was not the rate-determining step for the whole adsorption process.

From the above results and discussion, it may be concluded that the application of GNPs for the removal of ASA, CAF, and APAP from an aqueous solution followed mainly pseudo-second-order kinetic model, as was confirmed by the convergence of the experimental data, the excellent correlation coefficients (>0.99), and the agreement between the calculated and experimental amounts adsorbed per unit mass of GNPs. Also, the removal process takes place in different steps, including liquid film diffusion and intra-particle diffusion, but none of these steps rate-determining. The adsorption mainly is due to the π–π electron donor–acceptor interaction between the ASA, CAF, and APAP molecules and GNPs.

Also, according to the above results and discussion, the adsorption capacities of ASA, CAF, and APAP by GNP at 296 K were 12.98 mg ASA/g GNP, 19.72 mg CAF/g GNP, and 18.07 mg APAP/g

GNP within 10 min at 293 K. These adsorption capacities were compared with other adsorption capacities reported in literatures. It worth to mention that to the best of the authors knowledge, no study focus on the adsorption/removal of ASA, CAF, and APAP together from solution, hence in this part a comparison for each pollutant was carried out. Carbon-based materials made from fly ash were used for acetaminophen adsorption and the maximum adsorption capacity obtained was 222 mg/g within 240 min [21]. Sepiolite was used as low cost adsorbent for the removal of caffeine and the equilibrium was reached in 10 days with adsorption capacity of 20.0 mg/g [22]. The adsorption of ASA from solution by natural zeolites and clays was studied and maximal adsorption capacity obtained for ASA was 2.1×10^{-5} mol/g (3.36 mg/g) at 303 K after 2 h [9]. In another study, molecularly imprinted polymers (MIPs) were used for the selective separation of acetaminophen and aspirin using supercritical fluid technology and the results showed maximum adsorption capacities of 200 μmol/g (30.2 mg/g) and 230 μmol/g (41.4 mg/g), respectively, within 120 min at 298 K [24]. In another study, different MIPs were used for the selective separation of aspirin, and the results showed maximum adsorption capacities of 54.0 μmol/g (9.72 mg/g) within 720 min at 298 K [25]. The adsorption of acetaminophen and other pharmaceutical compounds by silica, alumina, and Porapak P was studied with a hydrophobic medium and the results showed that the adsorption of acetaminophen was insignificant (no values were reported) [26,27]. Sorption and sorption-biodegradation of acetaminophen, caffeine, and other pharmaceutical compounds using soil/sediments was studied. The results showed that sorption of acetaminophen and caffeine was 30% and 76% was removed, respectively, using 100 g soil/sediments from 500 ml water samples spiked with 50 μg/l [28]. The adsorption of nine selected micropollutants (six pharmaceuticals, two pesticides, and one endocrine disruptor) in water using an activated carbon was studied [29]. According to the authors, more than 90% of the APAP and CAF were adsorbed from the solution by activated carbon within 240 min with equivalent adsorption capacities of 0.1 mg/g for both APAP, and CAF, at pH of 7.0 and 293 K. Granular activated carbon was used in another study for the removal of caffeine from aqueous solution and adsorption capacity of 190.9 mg/g was observed at 296 K within 90 min [30]. According to the above recent literature review, it obvious that the adsorption capacities observed in this study for ASA, CAF, and APAP by GNPs were; in general, much higher than the reported values, and more over the time required for the adsorption to reach equilibrium in this study was the fastest ever reported. This showed the efficiency of GNPs for the removal of ASA, CAF, and APAP from aqueous solution.

3.5. Thermodynamic studies

The feasibility and spontaneity of the process of ASA, CAF, and APAP adsorption by GNPs was studied by calculating thermodynamic parameters: Gibbs free energy change (ΔG), enthalpy change (ΔH), and entropy change (ΔS). The thermodynamic parameters were calculated from the variation of the thermodynamic distribution coefficient D with a change in temperature according to the equation [31]:

$$D = \frac{q_e}{C_e} \tag{7}$$

where q_e is the amount of ASA, CAF, and APAP adsorbed by GNPs, (mg/g) at equilibrium, and C_e is the equilibrium concentration of ASA, CAF, and APAP in the solution (mg/l). The ΔH and ΔS may be calculated according to the following equation [32]:

$$\ln D = \frac{\Delta S}{R} - \frac{\Delta H}{RT} \tag{8}$$

Plotting $\ln D$ vs. $1/T$ for the adsorption of ASA, CAF, and APAP by GNPs, straight lines were obtained, as is presented in Fig. 10. The ΔH and ΔS values were calculated from the slope and the intercept of the straight line, respectively. The ΔH values were negative; -5.42 kJ/mole, -46.6 kJ/mole, and -25.4 kJ/mole, for the adsorption of ASA, CAF, and APAP by GNPs from aqueous solution, respectively. The negative values confirm the exothermic nature of the adsorption of ASA, CAF, and APAP by GNPs, which explains the decrease in adsorption at higher temperatures. The magnitude of ΔH suggests a weak type of bonding between ASA, CAF, and APAP by GNPs, such as physical adsorption, rather than chemical adsorption. The negative values of ΔS, -13.1 J/mole K, -123.0 J/mole K, and -67.3 J/mole K, suggested a decrease in randomness at the GNP/solution interface during the adsorption of ASA, CAF, and APAP on the GNPs' surface. The negative entropy of the adsorption and immobilization of ASA, CAF, and APAP on the GNPs' surface may be attributed to the decrease in the degree of freedom of the pharmaceutical molecules.

The ΔG values were calculated at 296 K from the relation:

$$\Delta G = \Delta H - T\Delta S \qquad (9)$$

The free energy change, ΔG, was negative, as would be expected for a product-favored and spontaneous reaction. The negative values of ΔG; -1.54 kJ/mole, -10.2 kJ/mole, and -5.42 kJ/mole, represents the adsorption of ASA, CAF, and APAP by GNPs from aqueous solution, respectively. Generally, the negative values of ΔG, ΔH, and ΔS suggest that the removal process is an enthalpy-driven process. It is noteworthy that the ΔG values were representative of the adsorption behavior of ASA, CAF, and APAP by GNPs from aqueous solution, as is shown in Fig. 11. The more negative the ΔG, the more spontaneous the adsorption was; accordingly, a more negative ΔG was associated with a higher the percentage of adsorption or adsorption capacity. CAF had the highest percentage of adsorption at 98.6% at 296 K, followed by APAP with 90.3% at 296 K, and finally by ASA at 64.8% at 296 K. Their ΔG values were -10.2 kJ/mole, -5.42 kJ/mole, and -1.54 kJ/mole, respectively. Also, the same trend was observed for the ΔH: a more negative ΔH was associated with an increased adsorption of the pharmaceutical pollutants. This is presented in Fig. 11. One possible explanation for these phenomena might be the pK_a values of the pharmaceutical pollutants. At a solution pH of 8.0, only ASA molecules were ionized (pK_a is 3.5) which decreased the π–π interaction between the negatively charged ASA ions and the GNPs' surface; consequently, the percentage of adsorption decreased. Meanwhile,

Fig. 11. Correlation between adsorption (%) for ASA, CAF, and APAP adsorbed by GNPs, with different thermodynamic parameters, and the pK_a values. (Experimental conditions: 200.0 ml, pH 8.0, 4.0 mM KNO$_3$, 200.0 mg GNPs, and ASA, CAF, and APAP concentrations 20.0 g l^{-1}.)

both CAF (pK_a is 14.0) and APAP (pK_a is 9.9) exist as neutral molecules, and their π–π interaction with the GNPs reached its maximum; consequently, the percentage of adsorption increased.

4. Environmental applications

The applicability of GNPs to the removal of the selected pharmaceutical pollutants was explored using real environmental aqueous samples: tap water (TWS), wastewater (WWS), and Red Sea water (RSW). The concentrations of the three pollutants were measured initially and were found below the detection limit of the HPLC. Accordingly, the three real water samples were spiked with 0.2 ml concentrated solution of ASA, CAF, and APAP (1000 mg l^{-1}) was added to 10.0 ml of the real water samples to obtain final concentrations of 20 mg l^{-1}. Then the real samples were equilibrated overnight, and then the 10.0 mg of GNPs was added to the spiked samples and left for 60.0 min. Then the amount adsorbed was calculated by comparing the concentrations of the pharmaceutical pollutants before and after the adsorption. In general, most of the CAF and APAP were removed from the TWS, WWS, and RSWS spiked samples, whereas more than 80.0% of the ASA was removed. The percentage of ASA, CAF, and APAP removed were, respectively, 81.5%, 97.4%, and 95.5%, for the TWS, 87.7%, 98.1%, and 98.0%, for the WWS, and 80.0%, 96.4%, and 95.6% for the RSWS with concentration of 20 mg l^{-1}. In general, the adsorption of ASA, CAF, and APAP by GNPs from RSWS was slightly low compared with WWS and TWS. This is may be due to the high concentration of Na$^+$, Ca^{2+}, and Mg^{2+} in the sea water sample (Table 1), which compete with the ASA, CAF, and APAP for the adsorption on the GNPs binding sites. The same phenomenon was observed in previous studies [33,34]. Also, the low adsorption of ASA, CAF, and APAP by GNPs from TWS compared with WWS could be attributed to the higher pH value of the tap water. This confirms the applicability of GNPs for environmental remediation, especially in regard to pharmaceutical pollutants such as aspirin, acetaminophen, and caffeine.

5. Conclusions

The adsorption/removal behavior of aspirin, acetaminophen, and caffeine by high surface area graphene nanoplatelets from
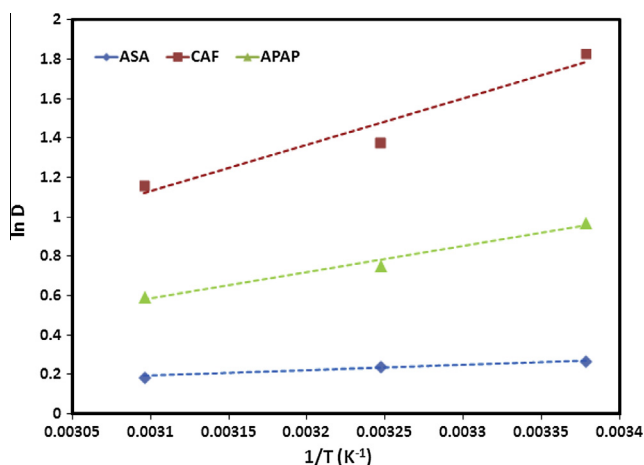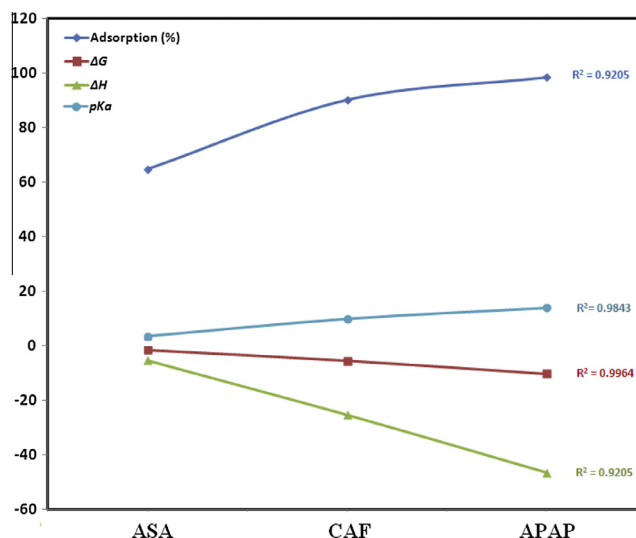

Fig. 10. Plot of $\ln D$ vs. $1/T$ for the estimation of thermodynamic parameters for ASA, CAF, and APAP adsorbed by GNPs. (Experimental conditions: 200.0 ml, pH 8.0, 4.0 mM KNO$_3$, 200.0 mg GNPs, and ASA, CAF, and APAP concentrations 20.0 mg l^{-1}.)

aqueous solutions was investigated. The effect of different environmental factors in the adsorption process was studied and the results revealed that most of the ASA, CAF, and APAP could be removed using 10.0 mg GNPs, after 10.0 min, at 296 K, and in solutions with a pH of 8.0. The adsorption was studied kinetically and the experimental data were best fitted using the pseudo-second-order kinetic model, which provided excellent correlation coefficients and agreement between the experimental adsorption capacities and the calculated one. The adsorption capacities for ASA, CAF, and APAP were 12.98 mg/g, 19.72 mg/g, and 18.07 mg/g at 296 K, respectively. The adsorption capacities decreased in inverse relationship to solution temperature, indicating the exothermic nature of the adsorption process. The experimental data were fitted by intra-particle diffusion and liquid film diffusion models in order to determine the rate-determining step of the removal process; the fitting occurred only for a part of the adsorption, indicating that none of the models control the adsorption process solely. The thermodynamics study of the adsorption process showed the spontaneity of the adsorption since the $\Delta G°$ values were negative; ΔG values were −10.2 kJ/mole, −5.42 kJ/mole, and −1.54 kJ/mole, for the adsorption of ASA, CAF, and APAP, respectively. The adsorption process was exothermic in nature with negative $\Delta H°$ values; these were −5.42 kJ/mole, −46.6 kJ/mole, and −25.4 kJ/mole for the adsorption of ASA, CAF, and APAP, respectively. The negative values of ΔS, −13.1 J/mole K, −123.0 J/mole K, and −67.3 J/mole K for ASA, CAF, and APAP, respectively, were due to the decrease in the degree of freedom resulting from the immobilization of pollutant molecules on the GNPs' surface. Finally, GNPs were used successfully for the removal of the ASA, CAF, and APAP from spiked tap water, waste water, and sea water with high efficiencies.

References

[1] J.L. Rodríguez-Gil, M. Catalá, S.G. Alonso, R.R. Maroto, Y. Valcárcel, Y. Segura, R. Molina, J.A. Melero, F. Martínez, Heterogeneous photo-Fenton treatment for the reduction of pharmaceutical contamination in Madrid rivers and ecotoxicological evaluation by a miniaturized fern spores bioassay, Chemosphere 80 (2010) 381–388.

[2] J.L. Santos, I. Aparicio, E. Alonso, Occurrence and risk assessment of pharmaceutically active compounds in wastewater treatment plants, A case study: seville city (Spain), Environ. Inter. 33 (2010) 596–601.

[3] Y. Kaya, G. Ersan, I. Vergili, Z.B. Gndera, G. Yilmaz, N. Dizge, C. Aydiner, The treatment of pharmaceutical wastewater using in a submerged membrane bioreactor under different sludge retention times, J. Membrane Sci. 442 (2013) 72–82.

[4] J. Radjenovića, M. Petrovića, D. Barcelóa, Fate and distribution of pharmaceuticals in wastewater and sewage sludge of the conventional activated sludge (CAS) and advanced membrane bioreactor (MBR) treatment, Water Res. 43 (2009) 831–841.

[5] Y. Li, G. Zhu, W.J. Ng, S.K. Tan, A review on removing pharmaceutical contaminants from wastewater by constructed wetlands: design, performance and mechanism, Sci. Total Environ. 468–469 (2014) 908–932.

[6] F. Martínez, M.J. López-Muñoz, J. Aguado, J.A. Melero, J. Arsuaga, A. Sotto, R. Molina, Y. Segura, M.I. Pariente, A. Revilla, L. Cerro, G. Carenas, Coupling membrane separation and photocatalytic oxidation processes for the degradation of pharmaceutical pollutants, Water Res. 47 (2013) 5647–5658.

[7] Q. Dai, J. Wang, J. Yu, J. Chen, J. Chen, Catalytic ozonation for the degradation of acetylsalicylic acid in aqueous solution by magnetic CeO$_2$ nanometer catalyst particles, Appl. Catal. B: Environ. 144 (2014) 686–693.

[8] J.L. Sotelo, A. Rodríguez, S. Álvarez, J. García, Removal of caffeine and diclofenac on activated carbon in fixed bed column, Chem. Eng. Res. Des. 90 (2012) 967–974.

[9] V. Rakić, N. Rajić, A. Daković, A. Auroux, The adsorption of salicylic acid, acetylsalicylic acid and atenolol from aqueous solutions onto natural zeolites and clays: clinoptilolite, bentonite and kaolin, Micropor. Mesopor. Mater. 166 (2013) 185–194.

[10] N. Bolong, A.F. Ismail, M.R. Salim, T. Matsuura, A review of the effects of emerging contaminants in wastewater and options for their removal, Desalination 239 (2009) 229–246.

[11] S. Wang, H. Sun, H.M. Ang, M.O. Tadé, Adsorptive remediation of environmental pollutants using novel graphene-based nanomaterials, Chem. Eng. J. 226 (2013) 336–347.

[12] X. Yuan, Y. Wang, J. Wang, C. Zhou, Q. Tang, X. Rao, Calcined graphene/MgAl-layered double hydroxides for enhanced Cr(VI) removal, Chem. Eng. J. 221 (2013) 204–213.

[13] H. Wang, X. Yuan, Y. Wu, H. Huang, G. Zeng, Y. Liu, X. Wang, N. Lin, Y. Qi, Adsorption characteristics and behaviors of graphene oxide for Zn(II) removal from aqueous solution, Appl. Surf. Sci. 279 (2013) 432–440.

[14] L. Ai, J. Jiang, Removal of methylene blue from aqueous solution with self-assembled cylindrical graphene–carbon nanotube hybrid, Chem. Eng. J. 192 (2012) 156–163.

[15] J.-S. Cheng, J. Du, W. Zhu, Facile synthesis of three-dimensional chitosan–graphene mesostructures for reactive black 5 removal, Carbohyd. Polym. 88 (2012) 61–67.

[16] J Rouquerol, F. Rouquerol, P. Llewellyn, G. Maurin, K.S.W. Sing, Adsorption by powders and porous solids: principles, Methodology and Applications, Academic Press, 2013. p. 166.

[17] Rosy, S.K. Yadav, B. Agrawal, M. Oyama, R.N. Goyal, Graphene modified Palladium sensor for electrochemical analysis of norepinephrine in pharmaceuticals and biological fluids, Electrochim. Acta (2014).

[18] D.D. Eley, Herman Pines, Paul Burg Weisz, Adv. Catal. Technol. Eng. 39 (1993) 424.

[19] H.J. Rhodes, J.J. Denardo, D.W. Bode, M.I. Blake, Differentiating nonaqueous titration of aspirin, acetaminophen, and salicylamide mixtures, J. Pharma. Sci. 75 (1975) 1386–1388.

[20] Y.S. Ho, Review of second-order models for adsorption systems, J. Hazard. Mater. 136 (2006) 681–689.

[21] M. Galhetas, A.S. Mestre, M.L. Pinto, I. Gulyurtlu, H. Lopes, A.P. Carvalho, Carbon-based materials prepared from pine gasification residues for acetaminophen adsorption Chem, Eng. J. 240 (2014) 344–351.

[22] S. Álvarez, J.L. Sotelo, G. Ovejero, A. Rodríguez, J. García, Low-cost adsorbent for emerging contaminant removal in fixed-bed columns, Chem. Eng. Trans. 32 (2013) 61–66.

[23] J. Acharya, J.N. Sahu, C.R. Mohanty, B.C. Meikap, Removal of lead (II) from wastewater by activated carbon developed from Tamarind wood by zinc chloride activation, Chem. Eng. J. 149 (1–3) (2009) 249–262.

[24] S.-D. Yoon, H.-S. Byun, Molecularly imprinted polymers for selective separation of acetaminophen and aspirin by using supercritical fluid technology, Chem. Eng. J. 226 (2013) 171–180.

[25] H.-S. Byun, Y.-N. Youn, Y.-H. Yun, S.-D. Yoon, Selective separation of aspirin using molecularly imprinted polymers, Sep. Purif. Technol. 74 (2010) 144–153.

[26] O. Lorphensri, J. Intravijit, D.A. Sabatini, T.C.G. Kibbey, K. Osathaphan, C. Saiwan, Sorption of acetaminophen, 17α-ethynyl estradiol, nalidixic acid, and norfloxacin to silica, alumina, and a hydrophobic medium, Water Res. 40 (2006) 1481–1491.

[27] O. Lorphensri, D.A. Sabatini, T.C.G. Kibbey, K. Osathaphan, C. Saiwan, Sorption and transport of acetaminophen, 17α-ethynyl estradiol, nalidixic acid with low organic content aquifer sand, Water Res. 41 (2007) 2180–2188.

[28] A.Y.-C. Lin, C.-A. Lin, H.-H. Tung, N.S. Chary, Potential for biodegradation and sorption of acetaminophen, caffeine, propranolol and acebutolol in lab-scale aqueous environments, J. Hazard. Mater. 183 (2010) 242–250.

[29] S.-W. Nam, D.-J. Choi, S.-K. Kim, N. Her, K.-D. Zoh, Adsorption characteristics of selected hydrophilic and hydrophobic micropollutants in water using activated carbon, J. Hazard. Mater. 270 (2014) 144–152.

[30] J.L. Sotelo, G. Ovejero, A. Rodríguez, S. Álvarez, J. Galán, J. García, Competitive adsorption studies of caffeine and diclofenac aqueous solutions by activated carbon, Chem. Eng. J. 240 (2014) 443–453.

[31] A. Ahatnagar, A.K. Minocha, B.H. Jeon, J.M. Park, Adsorptive removal of cobalt from aqueous solutions by utilizing industrial waste and its cement fixation, Sep. Sci. Technol. 42 (2007) 1255–1266.

[32] M. Abdel Salam, Coating carbon nanotubes with crystalline manganese dioxide nanoparticles and their application for lead ions removal from model and real water, Coll. Surf. A. 419 (2013) 69–79.

[33] R. Mandal, M.A. Salam, C.L. Chakrabarti, M. Back, An electrochemical investigation of complexation of Pb(II) by a well characterized fulvic acid in model systems-effect of competition with major cations and trace metals, Electroanalysis 15 (2003) 903–906.

[34] S.A. Kosa, G. Al-Zhrania, M. Abdel Salam, Removal of heavy metals from aqueous solutions by multi-walled carbon nanotubes modified with 8-hydroxyquinoline, Chem. Eng. J. 181–182 (2012) 159–168.